Available online at www.sciencedirect.com

ScienceDirect

materialstoday: PROCEEDINGS

Materials Today: Proceedings 2 (2015) 3864 – 3873

The Selected Papers of 10th International Conference on Physics of Advanced Materials, ICPAM-10

Heterogeneous Membranes Modified with Nanoparticles of Inorganic Ion-Exchangers for Whey Demineralization

Yuliya Dzyazko[a,*], Liudmyla Rozhdestveskaya[a], Yurii Zmievskii[b], Yurii Volfkovich[c], Valentin Sosenkin[c], Nadejda Nikolskaya[c], Sergey Vasilyuk[a], Valerii Myronchuk[b], Vladimir Belyakov[a]

[a]*V.I. Vernadskii Institute of General & Inorganic Chemistry of the NAS of Ukraine, Palladin Ave. 32/34, Kiev, 03142, Ukraine*
[b]*National University of Food Technologies of the MES of Ukraine, Vladimirskaya str. 48, Kiev, 01601, Ukraine*
[c]*A.N. Frumkin Institute of Physical Chemistry and Electrochemistry of the RAS, Leninskii Pr. 31, Moscow, 119071, Russia*

Abstract

Composite materials were obtained by modification of polymer ion exchange membranes with nanoparticles of zirconium hydrophosphate and hydrated zirconium dioxide. Empirical parameters related to porosity of the membranes and ion transport were proposed. Nanoparticles (4-20 nm) in clusters and channels of ion exchange polymer improve transport of counter-ions: transport number of cations increases from 0.46 to 0.78 under limiting current. The aggregates in non-transport pores are a barrier against organic matters. The composites were applied to whey electrodialysis. Current efficiency reaches 97 % for K^+, Na^+, Ca^{2+}, Mg^{2+} cations and 11-22 % for HPO_4^{2-} and $H_2PO_4^-$ anions.

Selection and peer-review under responsibility of the conference committee of the 10th International Conference on Physics of Advanced Materials

Keywords: Organic-inorganic membranes, electrodialysis, zirconium hydrophosphate, hydrated zirconium dioxide, nanoparticles.

1. Introduction

* Corresponding author. Tel.: +38-097-488-4937; fax: +38-044-424-0462.
E-mail address: dzyazko@ionc.kiev.ua

2214-7853
Selection and peer-review under responsibility of the conference committee of the 10th International Conference on Physics of Advanced Materials
doi:10.1016/j.matpr.2015.08.003

Electrodialysis, theory and practical application of which is considered in [1], are used for removal of toxic ions from liquid industrial wastes, particularly for regeneration of galvanic bath [2], production of drinking water [3], desalination of mine water [4], recovery of organic and inorganic acids from multicomponent solutions [5], production of salt concentrates [6] and for many other purposes. Electrodialytic separation is also applied to food industry, it is used, for instance, for whey desalination [7]. Polymer ion-exchange membranes, which are applied to electrodialysis [1-7], accumulate organics and microorganisms [8]. As a result, the separation is blocked.

The problem can be solved using organic-inorganic membranes. As known, polymer membranes, which contain inorganic nanoparticles, are stable against fouling during baromembrane separation [9]. Similar approach could be applied to ion exchange separators. However, the attention is focused on proton conductive organic-inorganic cation-exchange materials. The information about the membranes of this type for electrodialysis is rather limited: the composites were obtained by adding of metal oxide to polyethersulfone directly during the membrane formation [10]. Another approach is modification of the membranes, which are produced by industry, with nanoparticles of inorganic ion-exchanger [11]. This way allows us to incorporate single nanoparticles [12-14] or their aggregates [15]. Each type of the particles affects functional properties of the membranes, however, this problem was not researched. At last, organic-inorganic membranes were not applied to objects of biogenic origin.

The aim of the work is to establish interrelation between porous structure of ion exchange polymer matrix and functional properties of the membranes and to find out functions of inorganic particles, which are located in different pores of the matrix. This information is necessary in order to form required properties of the membranes. The composites were applied to whey electrodialysis, this liquid contains proteins, which poison the membranes.

Such inorganic ion-exchangers as zirconium hydrophosphate (ZHP) and hydrated zirconium dioxide (HZD) were chosen as fillers. ZHP is a weakly acidic ion-exchanger due to $(-O)_2PO_2H$ and $-0PO_3H_2$ groups; its maximal capacity is reached in neutral solutions [16]. HZD sorbs anions (An^-) mainly in acidic media:

$$-OH+HAn \leftrightarrow -OH_2^+An^-, \quad (1)$$

and cations (Cat) from alkaline solutions:

$$-O^-H^+ + Cat^+ \leftrightarrow -O^-Cat^+ + H^+, \quad (2)$$

Isoelectric point is reached, as a rule, in neutral media: under these conditions cation- and anion exchange capacities are equal. Functional properties of the membranes are determined by ion-exchange ability of the filler.

2. Experimental

2.1. Modification of ion exchange materials with inorganic constituents

Heterogeneous MC-40 cation exchange and MA-40 anion exchange membranes (Schekinoazot, RF), a thickness of which in a swollen state is about 600 μm, were investigated. The cation-exchange membrane (further CM) was produced from CU-2 ion-exchange gel-like resin (65 mass %) containing $-SO_3H$ groups. The anion-exchange membrane (further AM) was made of EDE-10P anion-exchange resin (55 mass %), which contains $-NR_3^+$, =NH and $-NR_2$ groups.

The procedure of the CM modification involved following stages: (i) impregnation of the membrane (its area was 25 cm^3) with water for swelling; (ii) impregnation of the wet membrane with a 1 M $ZrOCl_2$ solution for 24 h at 298 K (a volume of the solution was 25 cm^3); (iii) multiple washing with a 0.01 M HCl solution up to pH 2 of the effluent for removal of additionally sorbed electrolyte (a volume of each portion of acid solution was 250 cm^3); (iv) treatment of the resin with a 1 M H_3PO_4 solution (25 cm^3) at 298 K; (v) multiple washing with deionized water; (vi) drying in a desiccator over $CaCl_2$ at 298 K down to constant mass; (vii) treatment of the sample with ultrasound at 30 kHz using a Bandelin device (Bandelin Electronic) for cleaning, (vii) drying in a desiccator, (iv) weighting and storage in deionized water.

The procedure of the AM modification was similar to that described above. However, the (ii) stage involved impregnation of the membrane with a 1 M NH_4OH solution, deionized water was used for washing in (iii) stage, the sample washed down to pH 8 of the effluent. Further a 1 M $ZrOCl_2$ solution was used to precipitate HZD ((iv) stage).

As found, the amount of ZHP in the CM and HZD in the AM was 5.7 and 4.5 mass %. Modification of CU-2 and

EDE-10P granulated ion-exchangers was performed by a similar manner.

2.2. Morphology of the ion-exchange materials

SEM images of cross-sections of the membranes were obtained by means of a JEOL JSM 6700 F and JEOL JFC-1600 scanning electron microscopes (Jeol). A platinum layer was deposited onto the membrane surface at 3 Pa using an JEOL JFC-1600 Auto fine coater (Jeol). TEM image of the modified ion-exchange resin (preliminary crashed and treated with ultrasound) was obtained with a JEOL JEM 1230 transmission electron microscope (Jeol).

The method of standard contact porosimetry [17] was applied to the membranes, porous structure of which is formed during swelling. Preliminary the samples were vacuumized at 343 K. Water was used as a working liquid.

2.3. Characterization of the membranes and whey electrodialysis

Two-compartment cell supplied with platinum electrodes was used for measurements of electrical resistance of the membranes. The compartments were filled with NaCl solutions of equal concentration (1-40 mol m^{-3}). The measurements were carried out using an Autolab impedance system in a frequency interval of 10^{-2}-10^{6} Hz, the cell resistance was determined as a wide plateau of frequency dependence of the real part of impedance. The membrane resistance was calculated as a difference between resistances of the cell with and without membrane [18].

Voltammetric measurements were performed according to four-electrode scheme [19], which involved two-compartment, two platinum working electrodes (connected with a power supplier and ammeter) and two Ag/AgCl electrode connected with a voltmeter. The equipment is listed in [20]. The reference electrodes were supplied with Luggin capillaries, which defined a clear sensing point for the reference electrode near the two sides of the membrane. An effective membrane area was 4 cm^2, a distance between the membrane and each working electrode was 4 cm, a cross-section area of each compartment was 16 cm^2. A neutral NaCl solution (40 mol m^{-3}) was passed through each compartment with a flow velocity of 3 cm^3 s^{-1} using 2 centrifugal pumps.

Experimental set-up involved three-compartment divided cell, two independent liquid lines, power supplier and measuring instrumentation mentioned above. A scheme of the membrane system was as follows: cathode compartment – CM – desalination compartment – AM – anode compartment. Pairs of pristine or composite membranes were used. Geometrical parameters of the cell were similar to those listed in [20]. Whey (1.5 dm^3) circulated through the desalination compartment with a flow velocity of 5 cm^3 s^{-1} (first line). A 0.1 M HCl solution (1.5 dm^3) circulated through the cathode and anode compartment (second line).

Electrodialysis was performed at 20 mA. The content of Ca^{2+} and Mg^{2+} ions in the concentrate was determined by means of atomic absorption method using a Pye Unicam 8800 UV/VIS device (Philips), concentration of K^+ and Na^+ ions was analysed using a PFM-U4.2 flame photometer (Analitprylad, Ukraine). Phosphorus content was determined as molibdovanadophosphoric acid [21] with a Shimadzu UV-mini 1240 spectrophotometer (Shimadzu).

3. Results and discussion

3.1. Visualization of the inorganic constituent

As known, porous structure of swollen ion-exchange membranes involves a system of transport pores, where functional groups are placed [22]. The transport pores are a system of nanosized clusters and channels between them. Hydrophobic fields of hydrocarbonaceous chains form larger pores. Since these voids are free from functional groups, a liquid inside them contain both counter- and co-ions. Porous structure of heterogeneous membranes involves also structural defects and voids between the polymer and binder.

Impregnation of the cation-exchange resin with a $ZrOCl_2$ solution followed by treatment with phosphoric acid causes deposition of the non-aggregated nanoparticles (4-20 nm) inside the polymer matrix [12,13]. They are evidently stabilized by walls of the transport pores. The aggregates (up to 100 nm), which are located outside transport pores, have been also found. In the case of anion-exchanger, single nanoparticles as well as the aggregates are visible in the TEM image (Fig. 1a).

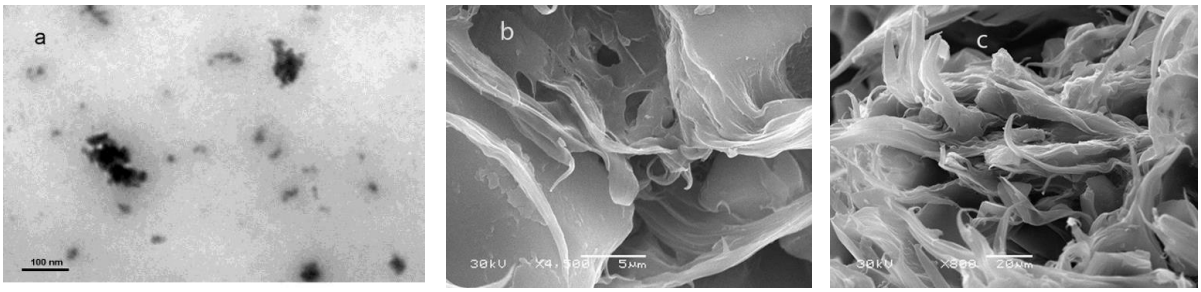

Fig. 1. TEM (a) and SEM (b, c) images of modified anion-exchange resin (a), composite cation-exchange membranes (b, c), where structure defects (b) as well as pores between the ion-exchange polymer and binder (c) are visible.

Similar regularities of deposition of the inorganic constituents are undoubtedly characteristic for the membranes. The cation-exchange membrane evidently contains both non-aggregated nanoparticles and their small aggregates. Some aggregates of micron size are visible in SEM image (Fig. 1b), they are placed in structure defects of the ion exchange polymer constituent of the heterogeneous membrane. No aggregates of comparable size are seen inside pores between the polymer and binder (Fig. 1c).

3.2. Porosity of the membranes

Both bulk and particle density tend to increase (cation-exchange membrane) and decrease (anion-exchange one) after modification (Table 1). Total porosity of the pristine and modified membranes is practically the same. Since the conditions of thermal pretreatment before the measurements cannot provide dehydration of the inorganic filler, the results are related only to the polymer. Several half-waves are visible in integral pore size distributions, which are plotted as dependencies of pore volume (V) *vs* pore radius (r) (insertions of Fig. 2). An area of each peak of differential distributions (Fig. 2) corresponds to a volume of each type of pores. Micropores (intersection of the integral plot with the ordinate axis) as well as small pores (r =2.5 nm) evidently correspond to channels. Pores, radii of which are 16 and 40 nm, are related to clusters and voids outside them respectively. Pores at r =630 -1000 nm are attributed to structure defects. The largest pores are between the ion-exchange polymer and binder.

Table 1. Density, porosity and specific surface area of the membranes

Sample	Density (cm^3g^{-1})		Porosity		Specific surface area per weight unit ($cm^2\ g^{-1}$)		Specific surface area per volume unit ($cm^2\ cm^{-3}$)	
	bulk	particle	micropores	total	micropores	total	micropores	total
pristine CM	0.69	1.33	0.23	0.47	485	560	333	392
composite CM	0.71	1.34	0.22	0.47	459	542	325	384
pristine AM	0.68	1.15	0.14	0.41	291	374	197	253
composite AM	0.66	1.11	0.12	0.40	265	345	176	229

A decrease of specific surface area per mass unit due to micropores (6 and 9 mass % for the CM and AM respectively) for the composites in a comparison with pristine membranes is higher than a content of the inorganic constituents indicating a change of swelling of the modified polymer. Regarding the CM, a decrease of porosity due to clusters and non-transport pores is compensated by a growth of volume of macropores of micron size. Modification of the AM causes a decrease of volume of cluster, channels and structure defects. A volume of pores at r =40 nm increases, the porosity caused by voids between the ion-exchange polymer and binder also grows.

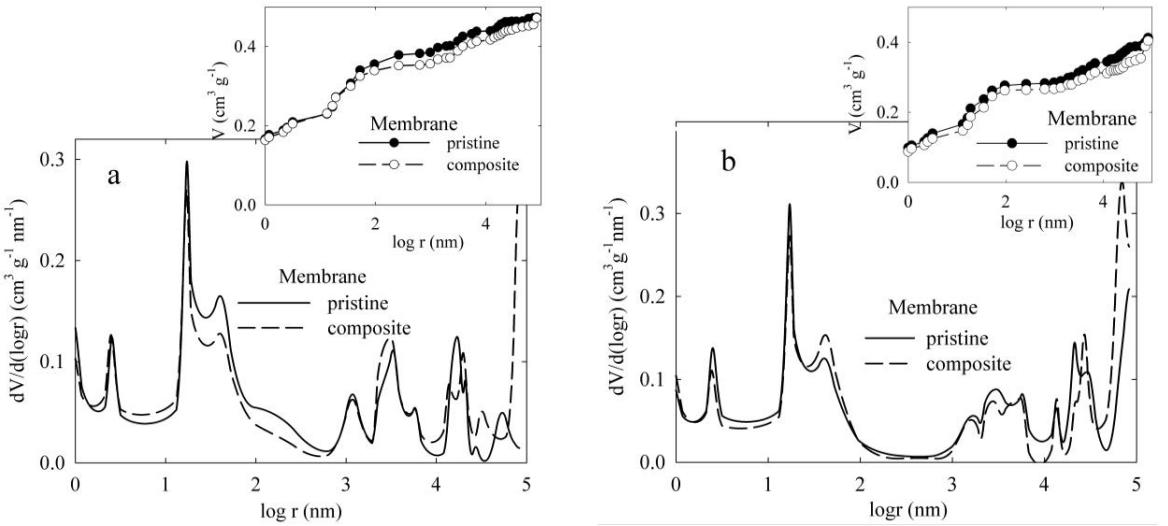

Fig. 2. Differential pore size distributions for the pristine and composite cation-(a) and anion-(b) exchange membranes. Insertions are the integral pore size distributions.

Based on results of TEM and SEM, it is possible to assume the influence of the inorganic constituent on porous structure of the composite membranes. Regarding the CM, the ZHP particles are placed in channels, clusters, non-transport pores and structure defects. They reinforce a tendency of the intraporous liquid to dilution (increase of volume of a certain type of pores). However this tendency is depressed by a partial screening of transport pores and pores with a radius of 40 nm with ZHP particles. Thus two mentioned effects are in a contradiction with each other. Hydration of structure defects of the composite CM is also reinforced by osmosis due to ZHP. Increase of porosity due to voids between the ion exchange polymer and binder can be rather a result of a growth of the polymer volume after modification. Indeed, the nanoparticles inside granulated ion-exchanger causes a growth of the grain size.

In the case of composite AM, osmosis is evidently insufficient, since isoelectric point of HZD is reached in neutral solutions [16]. Thus, a decrease of volume of the transport pores is mainly due to screening of clusters. This effect is also characteristic for structure defects. However, location of HZD in pores containing hydrophobic parts of hydrocarbon chains improves their hydrophilicity: a volume of pores at r =40 nm of the modified membrane is κ higher than those of the pristine membrane.

A change of porous structure of the modified membranes undoubtedly affects ion transport though them. This problem is considered further.

3.3. Electrical conductivity

Specific electrical conductivity of the membranes $(\bar{\kappa})$ is plotted in Fig. 3 as a dependence of the solution concentration (C). A decreasing of the C value causes reduction of the membrane conductivity, which involves also transport through clusters and channels (surface and fluid conductivity, if the diffusion parts of electric double layers (EDL) inside clusters are not overlapped). The fluid conductivity diminishes with a decreasing of concentration of the outer solution, a contribution of the surface conductivity into ion transport becomes stronger. At last, in the region, which corresponds to solution concentration of 2 - 1 mol m^{-3}, the conductivity increases evidently due to overlapping of the EDL in clusters (exclusion of fluid conductivity).

A radius of clusters can be calculated as [23]

$$r = \sqrt{\frac{\varepsilon_d \varepsilon_0 RT}{2F^2 C}} \tag{3}$$

where ε_0 is the dielectric permittivity of vacuum, ε is the dielectric constant (80 for water), R is the gas constant, F is the Faraday constant, T is the temperature, C is the concentration of outer solution, which corresponds to minimum of the $\overline{\kappa}$ - C curve (C=1 mol m^{-3}). A radius of the clusters was found to be 10 nm, this is in a good agreement with the data of porosimetric measurements (15 nm).

If the ion exchange membranes are in a contact with a solution of 1:1 electrolyte, their conductivity is determined as,

$$\overline{k} = F\left[\overline{u}_t \overline{C}_t + \overline{C}_{nt}\left(\overline{u}_{nt+} + \overline{u}_{nt-}\right)\right] \tag{4}$$

where $\overline{u}_t$ and $\overline{C}_t$ are the mobility and concentration of counter-ions in transport pores, $\overline{C}_{nt}$ is the electrolyte concentration in non-transport pores, $\overline{u}_{nt+}$ and $\overline{u}_{nt-}$ are the mobility of counter- and co-ions in non-transport pores. When $\overline{C}_{nt}(\overline{u}_{nt+} + \overline{u}_{nt-}) >> \overline{u}_t \overline{C}_t$, the electrolyte concentration in non-transport pores can be calculated as:

$$\overline{C}_{nt} = \frac{\overline{\kappa}}{F(\overline{u}_{nt+} + \overline{u}_{nt-})}. \tag{5}$$

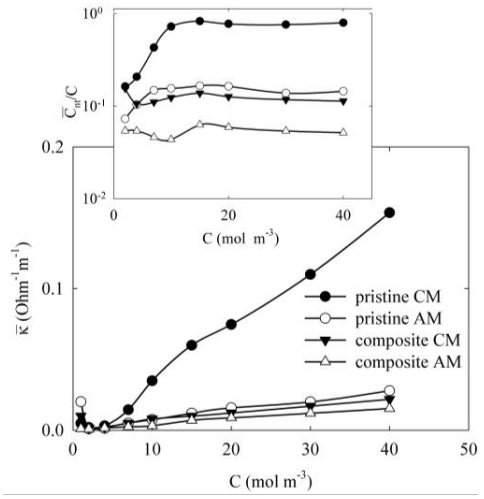

Fig. 3. Conductivity of membranes as a function of concentration of outer solution. Insertion − relation of concentrations of intraporous and outer solutions as a function of concentration of outer solution.

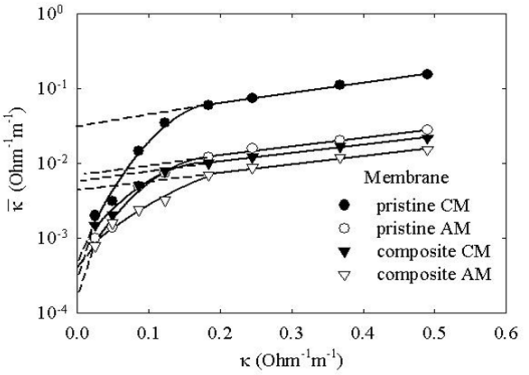

Fig. 4. Conductivity of membranes as a function of conductivity of outer solution.

A $\overline{C}_{nt} / C$ ratio is plotted in insertion of Fig. 3 as a function of concentration of outer solution. This ratio increases in the region of low concentrations (pristine membrane) or passes through slightly expressed minimum (composites) and further stabilizes. A minimum is probably caused by a screening effect of the inorganic particles in non-transport pores. The plateau corresponds to the concentration region, at which the conductivity is determined mainly by the electrolyte in non-transport pores.

The $\overline{\kappa} - \kappa$ plots (where κ is the conductivity of outer solution) are represented in Fig. 4 in semi-logarithmic coordinates (without the region, when the surface conductivity makes the greatest contribution into the $\overline{\kappa}$ value). Extrapolation of the curve to the ordinate axis gives a value, which corresponds to the ion transport only through clusters and channels (Table 2). These $\overline{\kappa}$ magnitudes are higher for the modified membranes due to participation of counter-ions of inorganic constituents in ion transport. Linear fields of $\log\overline{\kappa} - \kappa$ curves are related to the concentration, where the membrane conductivity is mainly due to the electrolyte in non-transport pores. Thus:

$$\log \overline{\kappa} = b_1 + b_2 \kappa \tag{6}$$

The b_1 parameter means logarithm of membrane conductivity, if $\kappa \to 0$ and a thickness of the EDL inside clusters is constant. The b_2 coefficient is a specific resistance of the outer solution, at which a difference of $\log \overline{\kappa} - b_1$ is equal to 1. The empirical coefficients characterize screening of the solution conductivity with the solid.

Table 2. Parameters, which characterize porous structure and functional properties of the membranes

Sample	b_1	b_2 (Ohm m)	$\overline{\kappa} \times 10^4$ ($\kappa \to 0$), (Ohm^{-1} m^{-1})	α	γ	$\overline{T}$ (i=i_{lim})
pristine CM	-1.46	1.33	5.62	1.85	1.59	0.46
composite CM	-2.19	1.10	6.97	1.76	1.50	0.78
pristine AM	-2.11	1.13	3.91	1.35	0.98	0.93
composite AM	-2.34	1.10	5.81	1.11	0.91	0.81

3.4. Interrelation between polymer porosity and membrane conductivity

Ion transport through the ion-exchange membranes is determined by a ratio of volumes of different types of pores [12, 13]. Earlier we have proposed the α parameter: it is a ratio of volumes of transport pores and pores, which are free from functional groups [12]. The movement of species through the cluster-channel system depends also on the content of bonded and free water. The mobility of species in bonded water (a thickness of its layer is 1.5 nm [19]) is rather low. Conversely, the mobility in boundary and free water is similar to that for a solution. The γ parameter, which is a ratio of smaller and larger transport pores, has been also proposed [12]. The mentioned characteristics were obtained using the data of the integral pore distributions and listed in Table 2. The α and γ parameters reflects the influence of polymer porosity on membrane conductivity at $\kappa \to 0$ and $\kappa > 0$ respectively.

The modified membranes show a decrease of the α and γ parameters in a comparison with the pristine materials. This means screening of transport pores, especially clusters and a growth of porosity caused by non-transport voids. However, a decrease of the b_1 and b_2 parameters shows transport of ions through pores between nanoparticles of the aggregates. The slowdown of ion transport is evidently due to aggregates, which are located in pores with a radius of 40 nm. Normally, ZHP is characterized by higher ion-exchange capacity in neutral media than HZD [16]. Thus, more significant decrease of the b_1 and b_2 values for the CM in a comparison with the AM is probably due to higher content of small aggregates or more compact packing of nanoparticles, which form these aggregates. Increase of the $\overline{\kappa}$ value, which corresponds to $\kappa \to 0$, is evidently due to particles in transport pores.

3.5. Voltammetry

Typical voltammetric curves for the membranes are given in Fig. 5.

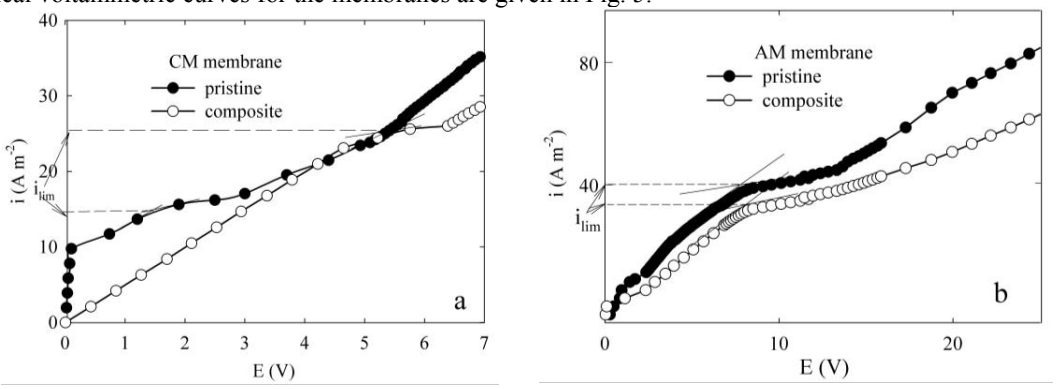

Fig. 5. Voltammetric curves for the pristine and modified cation- (a) and anion- (b) exchange membranes.

The first and second regions correspond to current, which is lower than the limiting value ($i_{\lim}$). The second one is related to concentration polarization (depletion of the solution at the solid-liquid interface in pores between the ion-exchange polymer and binder) at $i<0.75\, i_{\lim}$. This is typical for heterogeneous membranes [24]. The plateau is due to limiting current. Further growth of the current is attributed to overlimiting conditions, where the ion transport is due to also H^+ ions, which are formed during water split.

The voltammetric curve for the modified membrane is characterized by a linear region at $i\approx 0.75\, i_{\lim}$, it means no concentration polarization inside pores. Since no particles were found in the largest pores, their screening is due to small aggregates, which are located in pores with a radius of 40 nm. The aggregates prevent penetration of additionally sorbed counter- and co-ions inside pores between the ion exchange polymer and binder. The limiting current for the composite CM is higher than that for the pristine membrane. No concentration polarisation at $i<0.75 i_{\lim}$ is also observed for the composite AM, but the limiting current is lower in a comparison with pristine AM.

The limiting current is due to both migration and diffusion

$$i_{\lim} = \left(1+\left|z_{Cat}\right|/\left|z_{An}\right|\right) FkC \text{ [25].} \tag{7}$$

Here k is the mass transport coefficient, z is the charge number. Since the correlation equation is $Sh = 1.62\left(d\,\mathrm{Re}\,Sc/L\right)^{0.33}$ [26], where *Sh*, *Re*, *Sc* are the Sherwood, Reynolds and Schmidt criteria respectively, *d* and *L* are the distance between the membrane and electrode (0.04 m) and height of the compartment (0.04 m) respectively. The criteria are determined as $Sh = kd/D$, $Re = d\omega/\nu$, $Sc = \nu/D$, where *D* is the diffusion coefficient in a solution, ω is the superficial flow rate ($1.87\cdot10^{-2}$ m s^{-1}), ν is the kinematic viscosity (8.99 m^2 c^{-1} [27]). Thus, Sc = 691 (Na^+) and 449 (Cl^-), Sh =129 (Na^+) and 112 (Cl^-), Re =832. Thus, the mass transport coefficient was estimated as 4.19×10^{-6} (Na^+) and 5.60×10^{-6} (Cl^-) m s^{-1}. At last, we can calculate the effective transport number of species through the membrane at $i=i_{\lim}$:

$$\overline{T} = \frac{i_{\lim}}{\left(1+\dfrac{\left|z_{Cat}\right|}{\left|z_{An}\right|}\right)FkC}. \tag{8}$$

The $\overline{T}$ value for the modified CM is higher than for the pristine one due to screening of non-transport pores with ZHP aggregates, which form secondary membranes inside the polymer. HZD deteriorates charge selectivity evidently due to passage both cations and anions through the "secondary membrane". Indeed, isoelectric point is reached for HZD in neutral media. A contact of a one side of the membrane with acidic solution is necessary.

3.6. Electrodialysis testing

Table 3. Effective transport numbers obtained during whey desalination (i=0.75$i_{\lim}$=12.5 A m^{-2})

Membranes	Time (h)	K^+	Na^+	Ca^{2+}	Mg^{2+}	$\sum\overline{T}$, cations	$H_2PO_4^-$, HPO_4^{2-}
Pristine	1	0.347	0.056	0.058	0.010	0.471	0.102 – 0.275
	3	0.340	0.300	0.152	0.037	0.829	0.005 – 0.010
	5	0.182	0.386	0.292	0.017	0.877	0.033 – 0.066
Composite	1	0.364	0.203	0.148	0.081	0.796	0.011 – 0.023
	3	0.410	0.172	0.305	0.078	0.965	0.049 – 0.098
	5	0.440	0.134	0.328	0.073	0.975	0.114–0.221

Whey electrodialysis was performed at $i = 0.75\, i_{\lim}$. No sufficient decrease of amount of mineral components in whey was found during the process. The pH of the whey was about 6. Thus, a change of transport numbers reflects only membrane features and state of species in the liquid being purified. Fluxes of ions through each membranes ($\overline{N}$) were calculated as $dn/(Ad\tau)$ [26], where n is the amount of species in concentration compartments, A is the membrane area. The $\overline{T}$ values were determined as zFN/i [26] and given in Table 3. For $H_2PO_4^-$ and HPO_4^{2-}ions, z =1-2. Whey also contains Cl^- anions, however their transport was not investigated.

In general, the effective transport numbers of cations increases in time (except Mg^{2+}). The composite CM shows higher $\overline{T}$ value in a comparison with the pristine membrane. The modified AM demonstrates higher permittivity towards $H_2PO_4^-$ (HPO_4^{2-}) anions, their flux increases in time. The flux through the pristine AM decreases due to accumulation of organics.

Conclusions

The inorganic ion-exchange constituent is located in transport (non-aggregated nanoparticles) and non-transport (aggregates) pores of the polymer matrix. Due to osmotic and screening effects, the filler causes a change of pore volume. The aggregates form “secondary membranes” inside non-transport pores, this complicates penetration of additionally sorbed electrolyte inside the membrane. This prevents concentration polarization in pores, a size of which is larger than 10 μm. According to voltammetric measurements, the composite membranes behave like homogeneous separators.

In neutral media, charge selectivity of the “secondary membrane” is characteristic only for ZHP, which possesses considerable ion exchange capacity under these conditions. Insertion of this filler inside cation-exchange polymer results in an increase of transport numbers of counter ions. ZHD is able to exchange both cations and anions in neutral solutions. Its insertion into the AM deteriorates charge selectivity of the membrane in neutral media. Thus, a contact of a one side of the membrane with acidic solution is necessary.

The membranes were applied to whey desalination. In opposite to pristine membranes, which are poisoned with organics, fluxes of ions through composite separators increases in time. The current efficiency reaches 97 % for K^+, Na^+, Ca^{2+}, Mg^{2+} cations and 11-22 % for HPO_4^{2-} and $H_2PO_4^-$ anions. Ascertainment of the most suitable conditions of electrodialysis and :optimization of the stack configuration are necessary for further development of the process, which involves the composite membranes.

Acknowledgements

The work was supported by projects within the framework of programs supported by the National Academy of Science of Ukraine (entitled “Fundamental problems of creation of new matters and materials for chemical industry”, grant N 21-13), by the Ministry of Education and Science of Ukraine (entitled “Development of technology of purification of liquid food and industrial waste waters with membrane methods”, grant N 262-14).

References

[1] T. Sata, Ion exchange membranes. Preparation, characterization, modification and application, RSC, Cambridge, 2004.
[2] M.-L. Lameloise, R. Lewandowsky, J. Membr. Sci. 403-404 (2012) 196-202.
[3] Y. Tanaka, Desalination 301 (2012) 10-25.
[4] J. Hajduková, J. Thomas, P. Maliková, J. Vidlář, Adv. Mater. Res. 378-379 (2011) 414-417.
[5] X. Zhang, Ch. Li, X. Wang, Y. Wang, T. Xu, J. Membr. Sci. 409-410 (2012) 257-263.
[6] K. Himata, C. Warner, D. Currie, Q. Graves, G. Diachenko, J. Aqac. Intern. 88 (2005) 794-799.
[7] L. Diblíková, L. Čurda, K. Homolová, Desalination and Water Treatment, 14 (2010) 208-213.
[8] H.-J. Lee, M.-K. Hong, S.-D. Han, S.-H. Cho, S.-H. Moon, Desalination 238 (2009) 60-69.
[9] R. Pang, X. Li, J. Li, Z. Lu, X. Sun, L. Wang, Desalination 332 (2014) 60-66.
[10] Ch. Klaysom, Novel Organic-Inorganic Nanocomposite Membranes for Electrodialysis Application in Water Recovery, PhD Thesis, Australian Institute of Bioengineering and Nanotechnology, The University of Queensland, 2010.
[11] V. I. Zabolotskii, K. V. Protasov, M. V. Sharafan, Russ. J. Electrochem. 46 (2010) 979-986.
[12] Y. S. Dzyazko, L. N. Ponomaryova, Y. M. Volfkovich, V. E. Sosenkin, V. N. Belyakov, Separ. Sci. Technol. 48 (2012) 2140-2149.
[13] Y. S. Dzyaz'ko, L. N Ponomareva, Y. M. Vol'fkovich, V. E. Sosenkin, V.N. Belyakov. Russ. J. Electrochem. 49 (2013) 209-215.

[14] Y. S. Dzyazko, L. N. Ponomaryova, L. M. Rozhdestvenskaya, S. L. Vasilyuk, V. N. Belyakov, Desalination 342 (2014) 52-60.
[15] Y. S. Dzyazko, L. N. Ponomaryova, Y. M Volfkovich, V. V. Trachevskii, A. V. Palchik, Micropor. Mesopor. Mater. 198 (2014) 55-62.
[16] C. B. Amphlett, Inorganic Ion Exchangers, Elsevier, Amsterdam, 1964.
[17] Yu. M. Volfkovich, V. E. Sosenkin, V. S. Bagotzky, J. Power Sources, 195 (2010) 5429-5441.
[18] D. K. Hale, D. J. McCauley, Trans. Farad. Soc. 57 (1961) 135-149.
[19] N. P. Berezina, N. A. Kononenko, O. A. Dyomina, N. P. Gnusin, Advances in Colloid Interface Sci. 139 (2008) 3–28.
[20] Yu. S. Dzyazko, L. M. Rozhdestvenskaya, S. L. Vasilyuk, V. N. Belyakov, N. Kabay, M. Yuksel, O. Arar, U. Yuksel, Chem. Eng. Commun. 196 (2009) 22–38.
[21] K. P. Quinlan, M. A. DeSesa, Anal. Chem. 27 (1955) 1626–1629.
[22] V. I. Zabolotsky, V. V. Nikonenko, J. Membr. Sci. 79 (1993) 181–198.
[23] R. A. Robinson, R. H. Stokes, Electrolyte solutions, Dover, New York, 2002.
[24] O. V. Bobreshova, P. I. Kulintsov, E. M. Balavadze, J. Membr. Sci. 101 (1995) 1-12.
[25] K. J. Vetter, Electrochemishe Kinetik, Springer, Berlin, 1961.
[26] F. Walsh, A First Course in Electrochemical Engineering, Alresford Press, London, 1993.
[27] R. Parsons, Handbook of electrochemical constants, London, Butterworth Scientific Publications, 1959.